J Toxicol Pathol 2020; 33: 297–302

Case Report

Anaplastic nephroblastoma with peritoneal metastasis in an adult female Sprague Dawley rat

Lisa Quinn[1*], James G Fox[1], Joanna Joy[1], Sureshkumar Muthupalani[1], and Sebastian E Carrasco[1*]

[1] Division of Comparative Medicine, Massachusetts Institute of Technology, Cambridge, MA 02139, USA

Abstract: Spontaneous nephroblastomas are uncommon tumors of laboratory rats. This report describes a spontaneous nephroblastoma with peritoneal metastasis in an 11-month-old, female Sprague Dawley rat. The rat was part of a breeding program and presented 15 days post parturition with clinical signs including tachypnea, dyspnea and abdominal distension. At necropsy, the right kidney was markedly enlarged by an expansile pale-tan to white multinodular mass with extension into the retroperitoneal space, with multifocal variably sized nodules involving the mesentery, and surface of pancreas, liver, uterus, and ovarian bursa. The rat also had severe bicavitary effusion. Histologically, the renal parenchyma of the affected kidney was replaced by a moderately cellular, poorly-demarcated, non-encapsulated, multilobulated mass that appeared to compress the adjacent renal outer medulla and cortex. Three distinct neoplastic cell populations were identified in this renal tumor: epithelial cells (convoluted and dilated tubules / rare primitive glomeruloid structures), mesenchymal (neoplastic spindle cells in connective tissue), and blastemal cells (primitive neoplastic cells). The extrarenal nodular masses were predominantly composed of neoplastic mesenchymal and pleomorphic blastemal cells. Immunohistochemically, neoplastic epithelial cells in the renal mass were positive for pancytokeratin, and blastemal cells in both renal and extrarenal masses were positive for Wilms' tumor 1 protein (WT1) and vimentin. Neoplastic mesenchymal elements in both renal and extrarenal masses were positive for vimentin. The neoplasm was negative for chromogranin A and S100. The tumor was classified as an anaplastic nephroblastoma with metastasis to the mesentery and peritoneal organs. (DOI: 10.1293/tox.2020-0030; J Toxicol Pathol 2020; 33: 297–302)

Key words: nephroblastoma, renal neoplasm, peritoneal metastasis, Sprague Dawley rat, blastemal cells

Nephroblastoma is an uncommon spontaneous neoplasm in laboratory rats. This tumor has been sporadically reported in Noble (Nb), WAB/Not, Sprague Dawley, and Fisher 344 rats[1–3]. Additionally, this neoplasm occurs in both young and adult rats without sex preference[4]. Nephroblastomas are often unilateral and exhibit a rapid expansion throughout the entire renal parenchyma with occasional invasion of the renal capsule and surrounding connective tissues[4]. Metastasis of this tumor is rare but has been previously reported to metastasize to regional lymph nodes and lung[5–8]. This tumor in rats is considered an embryonal neoplasm originating from metanephric blastemal elements in the renal cortex[1, 4]. In most instances nephroblastomas exhibit a characteristic triphasic pattern consisting of epithelial, stromal and blastemal elements. Embryonal renal blastemal elements tend to form nests, islands, and cords of poorly differentiated cells, which often undergo epithelial differentiation giving rise the formation of glomerular, tubular and/or papillary cystic structures[4]. Unlike nephroblastomas in humans, neoplastic stromal components of neprhoblastomas in rats do not differentiate into vascular, cartilaginous, osseous and/or other tissues[4, 9, 10]. Neoplastic stromal elements in rat nephroblastomas occasionally exhibit rhabdomyocytic differentiation[11].

Nephroblastoma has also been induced experimentally by administering intraperitoneal injections of alkylating agents such as N-ethyl-N-nitrosourea (ENU) or N-methyl-N-nitrosourea (MNU) into dams, prenatal, or newborn rat pups[12–14]. Although this manipulation may also result in the formation of renal mesenchymal tumors, with careful histological and immunohistochemical analysis of the tumors, this model exhibits comparable immunohistological features with human neophroblastomas[15]. Additionally, nephroblastoma has been proven to be transplantable to F344 rats experimentally[16]. In this paper we describe a spontaneous nephroblastoma with metastasis to multiple peritoneal tissues in a rat. The 11-month-old female Sprague Dawley rat was housed at a research institution as part of a breeding program monitored and approved by the Institutional Animal Care and Use Committee and was experimentally naive. The lactating rat with the litter of pups were maintained in an autoclaved static caging system with beta

Received: 7 May 2020, Accepted: 20 July 2020
Published online in J-STAGE: 11 October 2020
*Corresponding authors: SE Carrasco (e-mail: scarrasc@mit.edu)
L Quinn (e-mail: quinnl@mit.edu)

chip bedding under pathogen-free conditions in a temperature-controlled room with a 12-hour light-dark cycle. Recent routine serological testing completed by Charles River on sentinel rats housed in the same room confirmed SPF conditions. The rats were provided autoclaved RO water and Formulab Diet 5008 LabDiet ad libitum. The rat displayed an acute onset of tachypnea with persistent lethargy and abdominal distension 15 days post parturition. On abdominal palpation, a large, firm, lobulated mass was detected. The rat had no history of experimental manipulation. Fifteen days prior the dam birthed a litter of pups which were all bright, alert, responsive and actively nursing from the dam but were also significantly undersized. Due to the declining condition of the dam, humane euthanasia was elected at this time, and the pups were successfully fostered onto another nursing dam within the breeding colony. The cross-fostered pups gained weight and were successfully weaned. Due to its poor prognosis, the rat was humanely euthanized with carbon dioxide and a diagnostic necropsy was performed. A bicavitary effusion was noted with pleural and peritoneal cavities containing 5.0 and 13 mls of serosanguinous fluid, respectively. The right kidney was markedly enlarged (~3.5 × 3.0 × 3.0 cm) by a pale-tan to white, multinodular, firm, infiltrative and non-encapsulated mass scattered throughout the renal cortex (Fig. 1A). The mass regionally invaded the renal capsule and adjacent retroperitoneal connective tissue in the caudal pole of the right kidney. The renal pelvis in this kidney was markedly dilated (hydronephrosis), and the contralateral kidney was grossly unremarkable.

The mesentery adjacent to the right kidney had multiple variably sized pale-tan nodules ranging from 0.4–2.0 cm in diameter. Secondary nodules were diffuse and adhered throughout the intestinal serosa, pancreas, mesenteric fat (Fig. 1B), hepatic capsule, uterus, and ovarian bursa.

Serum blood chemistry and complete blood cell count (CBC) both revealed several hematological parameters that were abnormal. The CBC differential revealed significant neutrophilia (4.7 K/uL), mild to moderate lymphopenia (3.1 K/uL), and mild monocytosis (0.6 K/UL) consistent with a stress leukogram. Mild anemia and dehydration were also observed (RBC 5.9 M/ul, hematocrit 42.5%, total protein of 5 g/dL). Serum chemistry revealed significant hypoalbuminemia (2.6 g/dL), elevated blood urea nitrogen (62 mg/dL), and moderate hypercholesterolemia (222 (mg/dL) which was suggestive of nephrotic syndrome. Urine was not collected in this case. Hyperglobuminemia (2.2 g/dL) was also observed which was likely secondary to neoplastic disease and/or lymphoid hyperplasia of lymphoid organs. AST (349 IU/L) was elevated likely due to myopathy as no histological lesions were noted in the liver.

Histopathology of the right kidney showed that the renal cortex and outer stripe medullary regions were replaced by a moderately cellular, non-encapsulated, multilobulated, expansile mass. The neoplasm was composed of three histologic components including; epithelial, mesenchymal and blastemal cells (Fig. 2A). The epithelial elements consisted of cuboidal to columnar epithelial cells arranged in primitive elongated, convoluted and/or dilated tubules surrounded by dense aggregates of blastemal cells (Fig. 2B). The neoplasm had convoluted ductular structures lined by cuboidal epithelial cells resembling the appearance of glomeruli (Fig. 2B) and rare glomeruloid-like structures (Fig. 2C). The mesenchymal elements consisted of spindle to stellate cells which were supported by an amphophilic to pale-eosinophilic fibrovascular stroma (Fig. 2A). The blastemal element consisted of polygonal to spindloid blastema cells arranged in islands, nests and dense aggregates, with scant to moderate basophilic cytoplasm. The cells had a round-oval to slightly elongated nuclei with prominent nucleoli. There was moderate to marked anisocytosis and anisokaryosis with an average of 7–8 mitotic figures per ten, 400× high power field (HPF; Fig. 2D). The inner and part of the outer stripe medulla had multifocal to coalescing areas of necrosis, with mixed clusters of cellular debris and erythrocytes

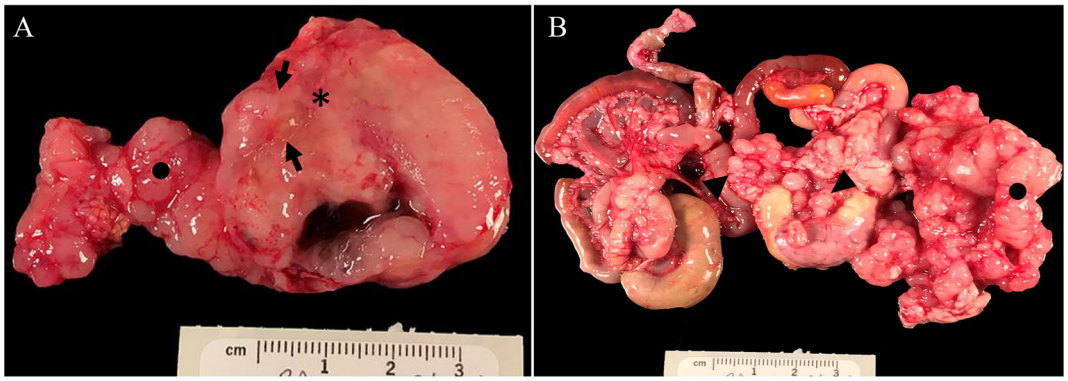

Fig. 1. Gross appearance of the tumor in the right kidney and mesentery from the rat. A) The right renal parenchyma was replaced by multifocal to coalescing pale-tan to white, firm to gelatinous nodules (arrows) completely effacing the corticomedullary junction (asterisk) and extending into the renal capsule. Additional neoplastic nodules adjacent to right renal mass were noted in the retroperitoneal space (circles). B) The mesentery was expanded by numerous variably-sized, pale-tan to white nodules (arrowheads) that often extended onto the serosal surface of the intestines.

and moderate amounts of pale-eosinophilic to amphophilic proteinaceous fluid.

The peritoneal nodules were predominantly composed by discohesive aggregates of pleomorphic blastemal cells, which were separated by short streams of spindle to stellate cells supported in a fibrovascular stroma (Fig. 2E). Blastemal elements in these nodules formed clusters of oval, spindloid to elongated basophilic cells with hyperchromatic nuclei and high nuclear to cytoplasm ratio (Fig 2F). Nuclei were oval to round with a prominent basophilic nucleolus. Blastemal cell exhibited moderate anisocytosis and marked anisokaryosis with high mitotic index averaging 7–8 mitotic figures per ten 400× high power field. No neoplastic epithelial components were noted within the peritoneal masses.

Immunohistochemistry (IHC) was performed for further characterization of the neoplasm (Table 1). Blastemal cells exhibited strong nuclear staining with Wilms' tumor 1 protein (WT1) (Rabbit Monoclonal, WT1/1434R, Dilution 1:200, NSJ Bioreagents, San Diego, CA, USA) in both the renal and peritoneal masses, (Fig. 3A and D). WT1 expres-

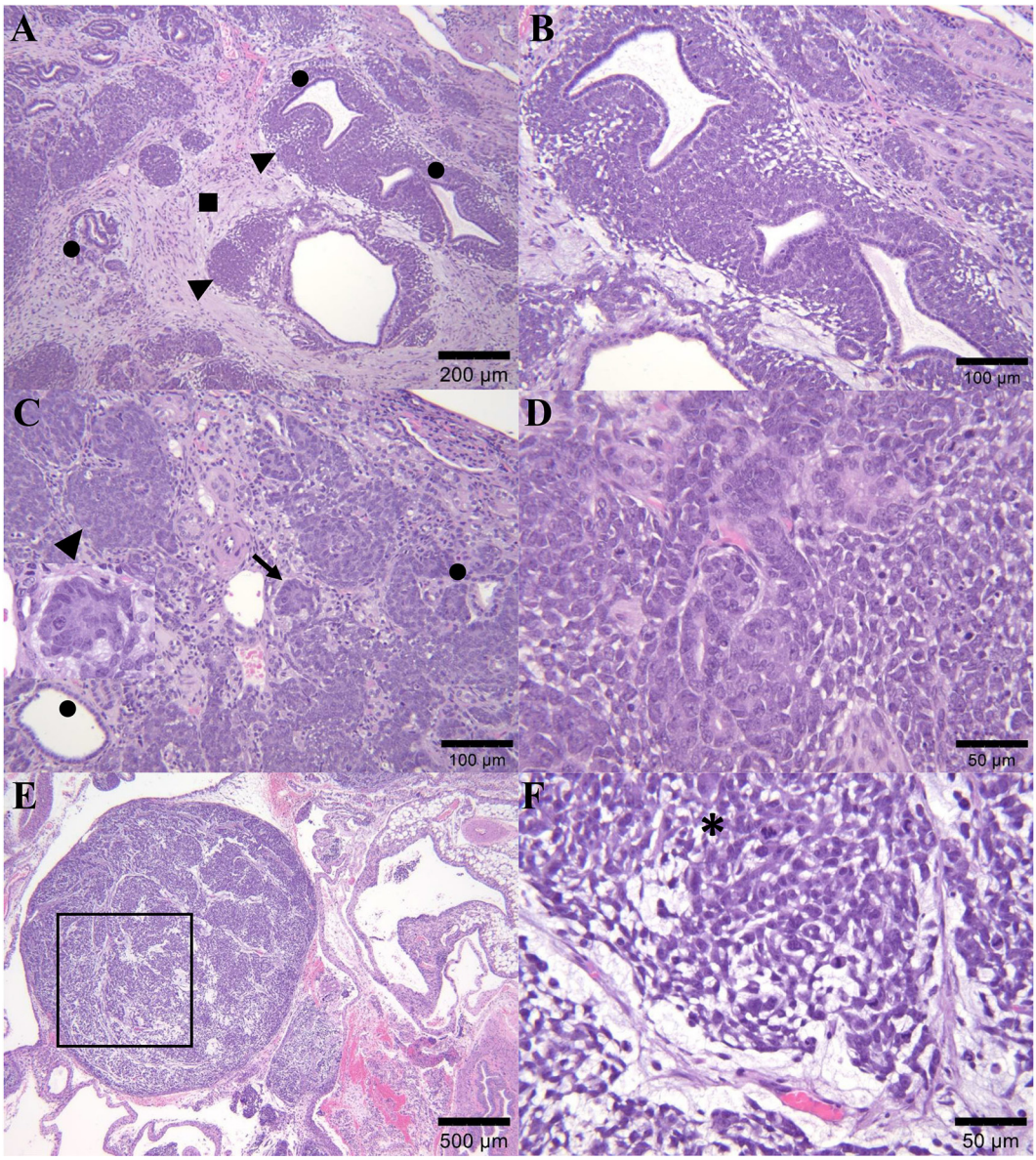

Fig. 2. Histopathological features of the nephroblastoma and peritoneal nodules. A) The right renal corticomedullary region was replaced by an infiltrative mass, composed of a mixture of three distinct neoplastic cell populations, including epithelial (circles), mesenchymal (square), and blastemal cells (arrowhead). B–C) Neoplastic epithelial cells were arranged in small tubules or elongated, convoluted and/or dilated tubules (circles), which were surrounded by blastemal cells (arrowhead). Glomeruloid-like structures (arrow and inset) were rarely present in the mass. D) Blastemal elements were often arranged in aggregates and lobules of closely-packed basophilic polygonal to spindloid primitive cells. E) The mesentery is expanded by well-demarcated, non-encapsulated, densely cellular multilobulated peritoneal nodules. F) Representative H&E image of a peritoneal nodule is comprised of dense clusters of blastemal cells (star) and separated by spindle to stellate cells in a fibrovascular stroma.

sion of blastemal cells was diffuse and specific throughout the neoplasm. The neoplastic mesenchymal and blastemal cells had strong cytoplasmic staining with vimentin in this neoplasm (Fig. 3B and E). Additionally, neoplastic tubular epithelial cells of the renal tumor exhibited cytoplasmic staining with pancytokeratin (Mouse Monoclonal AE1/AE3, Dilution 1:60, Biocare Medical, Pacheco, CA, USA). The peritoneal mass was negative for pancytokeratin as no tubular epithelial cells were found. (Fig. 3C and F) All neoplastic cells were negative for chromogranin A (Mouse Monoclonal, LK2H120, Dilution 1:50, Thermo Fisher Scientific, Waltham, MA, USA) as well as S100 (Mouse Monoclonal, 15E3E3, Dilution 1:100, Biocare Medical, Pacheco, CA, USA). The histological features of the neoplastic cells in both renal and extrarenal masses suggested that this tumor was a malignant nephroblastoma with pleomorphic and undifferentiated primitive (anaplasia) blastemal elements. Immunohistochemical staining of the renal mass supported the diagnosis of nephroblastoma given neoplastic cell populations were immunoreactive to WT1, vimentin and/or pancytokeratin. The extrarenal masses had biphasic pattern composed by blastemal cells and mesenchymal elements. Blastemal cells had variable degrees of differentiation and pleomorphism; features that have been previously reported in nephroblastomas in rats and Wilm's tumors in children[4, 9]. The gross appearance of the peritoneal nodules were an atypical feature as nephroblastomas in rats are more frequently reported to metastasize to the lung and regional lymph nodes[4, 5].

The differential diagnoses for this tumor included renal

Table 1. Immunohistochemical Staining of Neoplastic Cells in Renal and Peritoneal Mass

	Renal mass	Peritoneal mass
WT1*	+++	+++
Vimentin#	+++	+++
Pancytokeratin#	++	–
Chromogranin A	–	–
S100	–	–

*Nuclear expression of Wilms' tumor 1 protein (WT1) in blastemal cells, #Cytoplasmic expression of vimentin or AB1/AE2 keratins in neoplastic cells, +++ strong, ++ moderate, + mild, – negative.

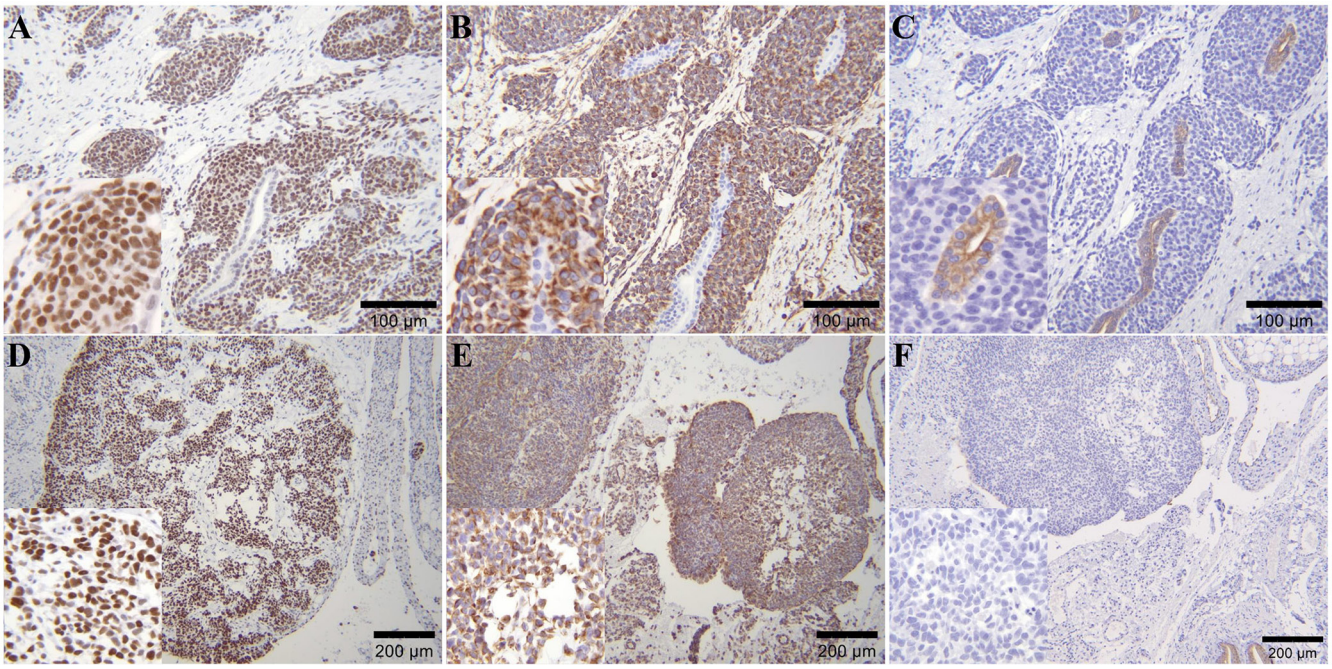

Fig. 3. Immunohistochemical staining of the right renal and mesenteric tumors. The IHC results of the renal mass are depicted in A–C. A) Wilms' tumor 1 protein (WT1) is detected in the nuclei of blastemal cells in the renal tumor. B) Vimentin was detected in the cytoplasm of blastemal and neoplastic mesenchymal cells in renal tumor. C) Pancytokeratin was detected in the cytoplasm of neoplastic epithelial cells in the renal tumor. Representative IHC results of the peritoneal tumors are depicted in D–F. D) Neoplastic blastemal cells in the peritoneal masses were positive for WT1 (nuclear staining). E) Blastemal and mesenchymal elements in peritoneal masses were positive for vimentin (cytoplasmic staining), F) Neoplastic cells in peritoneal tumors were negative for pancytokeratin.

carcinoma, renal mesenchymal tumor, and mesothelioma[5]. Renal carcinoma was ruled out as these neoplasms do not display a triphasic pattern and lack immunoreactivity for WT1[5]. Renal mesenchymal tumor was ruled out as these tumors are predominantly composed by neoplastic stromal and connective tissue elements and lack neoplastic epithelial cells[4,5]. Mesothelioma was excluded based on the histological features of the neoplastic blastemal cell population in peritoneal nodules. Mesotheliomas are often reported in Fisher 344 rats and form epithelial fronds or papillary structures (epithelioid subtype) and/or are composed of by bundles or whorls of neoplastic mesenchymal cells (sarcomatoid subtype)[17–20]. None of these histological features were noted in the renal tumor and peritoneal nodules. Additionally, peritoneal mesotheliomas are rarely reported in Sprague Dawley rats but occasionally this neoplasm has described within the thoracic cavity[21–24]. Based on the World Health Organization classification of mesotheliomas in humans, the nature of this tumor is confirmed using a variety of immunohistochemical markers, including pancytokeratin, vimentin, podoplanin, and calretinin[25]. Interestingly, pleural mesotheliomas in humans can exhibit immunoreactivity for WT1[25]. In comparison, mesothelial cells from malignant mesotheliomas in F344 rats are immunoreactive for mesothelin, podoplanin, vimentin, and pancytokeratins[26, 27]. Electron microscopy (EM) can be beneficial in the diagnosis of nephroblastomas but is not always essential due to the speed and accuracy of immunohistochemical staining[28]. When EM is completed it can aid in the diagnosis of nephroblastomas as neoplastic epithelial and blastemal cells exhibit junctional complexes and microvilli, are partially surrounded by basement membrane, and lack cytoplasmic vacuoles[4, 26].

In laboratory animal species, nephroblastoma tumors are most commonly reported in rats but have also been rarely reported in the cynomolgus macaque (*Macaca fasciularis*), baboon (*Papio sp.*), cotton-top tamarin (*Saguinus oedipus*), and common marmoset (*Callithrix jacchus*)[29–32]. Histopathologically, neophroblastomas in *Papio sp.* has been described to be similar as what is found in humans with anaplastic areas prevalent within the tumor as well as proliferative epithelial cells forming tubulars and aborted glomeruli. Also prominent were nephrogenic rests and proliferative fibrovascular tissue[30]. In humans, anaplastic nephroblastomas are associated with poorer prognosis and higher mortality rates than other histological subtypes. Genome sequencing analysis of Wilm's tumor, a form of nephroblastoma in children, identified several cancer genes that harbor likely oncogenic mutations, including epigenetic remodelers, microRNA processing genes, and transcription factors (SIX1 and SIX2)[33, 34]. Anaplastic subtypes of this tumor are often associated with somatic mutations in TP53[33]. These mutations are limited to anaplastic regions and are occasionally appreciated in other histologic subtypes. To our knowledge there is limited information on the molecular development of nephroblastoma in rats.

This case illustrates a primary spontaneous malignant nephroblastoma that exhibited anaplastic blastemal elements and atypical metastasis throughout peritoneum in a female Sprague Dawley rat. Blastemal elements in the renal mass and peritoneal nodules were characterized by poorly differentiated (anaplastic) and pleomorphic hyperchromatic primitive (blastemal) cells. Immunohistochemistry demonstrated the neoplasm had a triphasic pattern in the right kidney, and this pattern was useful to distinguish poorly differentiated blastemal elements in peritoneal nodules. Histopathology and IHC evaluation of this nephroblastoma suggest this tumor originated from metanephric blastemal elements in the renal medulla or cortex[4].

Disclosure of Potential Conflicts of Interest: The authors disclose receipt of the following financial support for the research, authorship, and/or publication of this article: This work was supported by the following National Institutes of Health grants P30-ES002109 (JGF) and T32-OD010978-30 (JGF).

Acknowledgements: We are very grateful to Joanna Richards and Caroline Atkinson for their work in the histology lab as well as Nancy McGilloway and the Boston College Animal Care Facility Staff. We would also like to thank Ellen Buckley at the Division of Comparative Medicine Diagnostic Laboratory for her assistance in hematological, clinical chemistry, and health surveillance testing.

References

1. Hard GC, Seely JC, and Betz LJ. A survey of mesenchyme-related tumors of the rat kidney in the national toxicology program archives, with particular reference to renal mesenchymal tumor. Toxicol Pathol. **44**: 848–855. 2016. [Medline] [CrossRef]
2. Middle JG, Robinson G, and Embleton MJ. Naturally arising tumors of the inbred WAB/Not rat strain. I. Classification, age and sex distribution, and transplantation behavior. J Natl Cancer Inst. **67**: 629–636. 1981. [Medline]
3. Hard GC, and Noble RL. Occurrence, transplantation, and histologic characteristics of nephroblastoma in the Nb hooded rat. Invest Urol. **18**: 371–376. 1981. [Medline]
4. Cardesa A, and Ribalta T. Nephroblastoma, kidney, rat. In: Urinary System. TC Jones, U Mohr, RD Hunt (eds). Springer, Berlin. 1986. 71–80.
5. Frazier KS, Seely JC, Hard GC, Betton G, Burnett R, Nakatsuji S, Nishikawa A, Durchfeld-Meyer B, and Bube A. Proliferative and nonproliferative lesions of the rat and mouse urinary system. Toxicol Pathol. **40**(Suppl): 14S–86S. 2012. [Medline] [CrossRef]
6. Cohen SM. Monographs on Pathology of Laboratory Animals, Vol. 2. Springer-Verlag Berlin, Heidelberg. 1998.
7. Ito Y, Matsushita K, Tsuchiya T, Kohara Y, Yoshikawa T, Sato M, Kitaura K, and Matsumoto S. Spontaneous nephroblastoma with lung metastasis in a rat. J Toxicol Pathol. **27**: 91–95. 2014. [Medline] [CrossRef]
8. Chandra M, Riley MG, and Johnson DE. Spontaneous renal neoplasms in rats. J Appl Toxicol. **13**: 109–116. 1993. [Medline] [CrossRef]

9. Fraizer GC, Eisermann K, Brett-Morris A, *et al.* Functional role of WT1 in prostate cancer. In: Wilms Tumor. van den Heuvel-Eibrink MM (ed). Codon Publications, Brisbane. 2016. 235–259.
10. Tanaka N, Izawa T, Yamate J, and Kuwamura M. Spontaneous nephroblastoma with striated muscle differentiation in an F344 rat. J Toxicol Pathol. **30**: 231–234. 2017. [Medline] [CrossRef]
11. Mesfin GM, and Breech KT. Rhabdomyocytic nephroblastoma (Wilms' tumor) in the Sprague-Dawley rat. Vet Pathol. **29**: 564–566. 1992. [Medline] [CrossRef]
12. Turusov VS, Alexandrov VA, and Timoshenko IV. Nephroblastoma and renal mesenchymal tumor induced in rats by N-nitrosoethyl- and N-nitrosomethylurea. Neoplasma. **27**: 229–235. 1980. [Medline]
13. Hard GC. Differential renal tumor response to N-ethylnitrosourea and dimethylnitrosamine in the Nb rat: basis for a new rodent model of nephroblastoma. Carcinogenesis. **6**: 1551–1558. 1985. [Medline] [CrossRef]
14. Diwan BA, and Rice JM. Effect of stage of development on frequency and pathogenesis of kidney tumors induced in Noble (Nb) rats exposed prenatally or neonatally to N-nitrosoethylurea. Carcinogenesis. **16**: 2023–2028. 1995. [Medline] [CrossRef]
15. Yoshizawa K, Kinoshita Y, Emoto Y, Kimura A, Uehara N, Yuri T, Shikata N, and Tsubura A. N-Methyl-N-nitrosourea-induced renal tumors in rats: Immunohistochemical comparison to human Wilms tumors. J Toxicol Pathol. **26**: 141–148. 2013. [Medline] [CrossRef]
16. Yamate J, Tajima M, Shibuya K, Saitoh T, and Kizaki H. Morphological characteristics of a transplantable nephroblastoma (NB-Y) in F344 rats and the relation of tumour growth to hyper-reninaemia in NB-Y-bearing rats. J Comp Pathol. **107**: 59–72. 1992. [Medline] [CrossRef]
17. Travis WD, Brambilla E, Nicholson AG, Yatabe Y, Austin JHM, Beasley MB, Chirieac LR, Dacic S, Duhig E, Flieder DB, Geisinger K, Hirsch FR, Ishikawa Y, Kerr KM, Noguchi M, Pelosi G, Powell CA, Tsao MS, Wistuba I. WHO Panel. The 2015 World Health Organization classification of lung tumors: impact of genetic, clinical and radiologic advances since the 2004 classification. J Thorac Oncol. **10**: 1243–1260. 2015. [Medline] [CrossRef]
18. Suzuki Y. Diagnostic criteria for human diffuse malignant mesothelioma. Acta Pathol Jpn. **42**: 767–786. 1992. [Medline]
19. Iwata H, Hirouchi Y, Koike Y, *et al* Historical control data of non neoplastic and neoplastic lesions in F344/DuCrj rats. J Toxicol Pathol. **4**: 1–24. 1991. [CrossRef]
20. Greaves P, Chouinard L, Ernst H, Mecklenburg L, Pruimboom-Brees IM, Rinke M, Rittinghausen S, Thibault S, Von Erichsen J, and Yoshida T. Proliferative and non-proliferative lesions of the rat and mouse soft tissue, skeletal muscle and mesothelium. J Toxicol Pathol. **26**(Suppl): 1S–26S. 2013. [Medline] [CrossRef]
21. Chandra M, Davis H, and Carlton WW. Naturally occurring atriocaval mesotheliomas in rats. J Comp Pathol. **109**: 433–437. 1993. [Medline] [CrossRef]
22. Peano S, Conz A, Carbonatto M, Goldstein J, and Nyska A. Atriocaval mesothelioma in a male Sprague-Dawley rat. Toxicol Pathol. **26**: 695–698. 1998. [Medline] [CrossRef]
23. Lewis DJ. Ovarian neoplasia in the Sprague-Dawley rat. Environ Health Perspect. **73**: 77–90. 1987. [Medline] [CrossRef]
24. Doi T, Kotani Y, Takahashi K, Hashimoto S, Yamada N, Kokoshima H, Tomonari Y, Wako Y, and Tsuchitani M. Malignant mesothelioma in the thoracic cavity of a Crj:CD(SD) rat characterized by round hyalinous stroma. J Toxicol Pathol. **23**: 103–106. 2010. [Medline] [CrossRef]
25. Husain AN, Colby TV, Ordóñez NG, Allen TC, Attanoos RL, Beasley MB, Butnor KJ, Chirieac LR, Churg AM, Dacic S, Galateau-Sallé F, Gibbs A, Gown AM, Krausz T, Litzky LA, Marchevsky A, Nicholson AG, Roggli VL, Sharma AK, Travis WD, Walts AE, and Wick MR. Guidelines for pathologic diagnosis of malignant mesothelioma 2017 update of the consensus statement from the international mesothelioma interest group. Arch Pathol Lab Med. **142**: 89–108. 2018. [Medline] [CrossRef]
26. Ohnuma-Koyama A, Yoshida T, Takahashi N, Akema S, Takeuchi-Kashimoto Y, Kuwahara M, Nagaike M, Inui K, Nakashima N, and Harada T. Malignant peritoneal mesothelioma with a sarcomatoid growth pattern and signet-ring-like structure in a female f344 rat. J Toxicol Pathol. **26**: 197–201. 2013. [Medline] [CrossRef]
27. Minami D, Takigawa N, Kato Y, Kudo K, Isozaki H, Hashida S, Harada D, Ochi N, Fujii M, Kubo T, Ohashi K, Sato A, Tanaka T, Hotta K, Tabata M, Toyooka S, Tanimoto M, and Kiura K. Downregulation of TBXAS1 in an iron-induced malignant mesothelioma model. Cancer Sci. **106**: 1296–1302. 2015. [Medline] [CrossRef]
28. Seely JC. Renal mesenchymal tumor vs nephroblastoma: Revisited. J Toxicol Pathol. **17**: 131–136. 2004. [CrossRef]
29. Zöller M, Mätz-Rensing K, Fahrion A, and Kaup FJ. Malignant nephroblastoma in a common marmoset (Callithrix jacchus). Vet Pathol. **45**: 80–84. 2008. [Medline] [CrossRef]
30. Goens SD, Moore CM, Brasky KM, Frost PA, Leland MM, and Hubbard GB. Nephroblastomatosis and nephroblastoma in nonhuman primates. J Med Primatol. **34**: 165–170. 2005. [Medline] [CrossRef]
31. Jones SR, and Casey HW. Primary renal tumors in nonhuman primates. Vet Pathol. **18**(Suppl 6): 89–104. 1981. [Medline] [CrossRef]
32. Bennett BT, Beluhan FZ, and Welsh TJ. Malignant nephroblastoma in Macaca fascicularis. Lab Anim Sci. **32**: 403–404. 1982. [Medline]
33. Treger TD, Chowdhury T, Pritchard-Jones K, and Behjati S. The genetic changes of Wilms tumour. Nat Rev Nephrol. **15**: 240–251. 2019. [Medline] [CrossRef]
34. Royer-Pokora B, Weirich A, Schumacher V, Uschkereit C, Beier M, Leuschner I, Graf N, Autschbach F, Schneider D, and von Harrach M. Clinical relevance of mutations in the Wilms tumor suppressor 1 gene WT1 and the cadherin-associated protein beta1 gene CTNNB1 for patients with Wilms tumors: results of long-term surveillance of 71 patients from International Society of Pediatric Oncology Study 9/Society for Pediatric Oncology. Cancer. **113**: 1080–1089. 2008. [Medline] [CrossRef]